Accelerating action of Alzheimer's disease gut microbiota on Tau protein hyperphosphorylation: crosstalk of inflammation and autophagy

Guo Yinrui
School of Basic Medical Science, Guangzhou University of Chinese Medicine
Tang Xiaocui
Guangdong Institute of Microbiology, Guangdong Academy of Sciences
Qi Longkai
Guangdong Institute of Microbiology, Guangdong Academy of Sciences
Yang Xin
The Fifth Affiliated Hospital of Guangzhou Medical University
Li Ran
Department of Physiology, Shantou University Medical College
Zhu Xiangxiang
Academy of Life Sciences, Jinan University, Guangdong Province
Zeng Miao
Chengdu University of Traditional Chinese Medicine
Deng Tianming
The Fifth Affiliated Hospital of Guangzhou Medical University
Fu Yonghong
Deparment of Intensive Care Unit, Guangzhou First People's Hospital; School of Medicine, South China University of Technology
Xie Yizhen
Guangdong Institute of Microbiology,
Wang Jian
School of Basic Medical Science, Guangzhou University of Chinese Medicine
Diling Chen (diling1983@163.com)
Guangdong Institute of Microbiology

Research

Keywords: Alzheimer's disease, Gut microbiota, Fecal microbiota transplantation, Tau protein hyperphosphorylation, Gut-brain axis

Posted Date: June 9th, 2020

DOI: https://doi.org/10.21203/rs.3.rs-32723/v1

Abstract

Background: The gut-brain axis has been implicated in the complex pathogenesis of Alzheimer's disease (AD), but the action is unclear, this study was performed to clarify the effect of ad-related gut microbiota on the pathogenesis of AD during pregnancy and early exposure.

Methods: A pilot study of gut microbiota in AD patients was performed.

Gut microbiota structure, long-term potentiation (LTP), inflammation levels, AD biomarkers, and metabolomics of serum and fecal were monitored after cohousing by cohousing in early life (from pregnancy 14 days to birth 14 days with 8-month old APP/PS1 mice).The regulatory action of bacterial metabolites on Tau protein phosphorylation was evaluated.

Results: Gut microbiota from APP/SP1 mice altered structure of gut microbiota in newborn mice, LTP in hippocampal slices was significantly shortened, and inflammatory markers levels were increased, AD biomarkers were upregulated, with significantly higher Tau protein phosphorylation at multiple sites ($p < 0.05$).

Conclusions: These results imply ad-related gut microbiota can change the structure of gut microbiota during pregnancy and early exposure. Changing the structure of gut microbiota in the newborn mice can induce leucine metabolism disorder, induce mTOR mediated autophagy dysfunction and increase the level of inflammation, thus leading to accelerate Tau protein phosphorylation and reduce LTP occurs in AD-cohousing mouse hippocampus.

Introduction

Gut microbiota interaction in diseases are becoming one of the most researched topics in life sciences. Exponential growth data revealed correlations between dysbacteriosis and several neurological diseases including autism[1], depression[2], Parkinson's disease (PD)[3], and Alzheimer's disease (AD) [4]Therefore, researchers have gradually shifted their focus from targeting the central nervous system to targeting the characteristics of gut microbiota and/or intestinal homeostasis.

There is a growing body of evidence that the central nervous system (CNS) regulates the gastrointestinal tract. In addition, it contains independent neural structures of the enteric nervous system, and the main nerve trunk containing the vagus, splanchnic, and sacral nerves connects the gastrointestinal tract and CNS[5]. More recent studies have revealed an interaction between the brain and gut, and their relationships have been defined as the gut-brain axis[1–5]. Another major way that gut microbiota regulate the brain is through the neuroimmune and neuroendocrine systems [6]. Intestinal microorganisms interact with intestinal endocrine cells (EECs), enterochromaffin cells (ECCs), and/or the intestinal mucosal immune system via cascading reactions with gut metabolites such as short-chain fatty acids (SCFAs), secondary bile acids (2Bas), and tryptophan[6]. Gut microbiota also produce substances that could stimulate neural tissues, such as γ-aminobutyric acid (GABA), norepinephrine,

dopamine, and serotonin that are directly or indirectly synthesized in the brain[7]. Although there are various communication pathways between the gut and brain, the precise regulation of these interactions is poorly understood.

With regard to intestinal neurodegenerative diseases, PD is the most deeply studied, and a series of breakthroughs have providing a basis for work in other neurodegenerative diseases. In 2016, scientists demonstrated a functional connection between the gut microbiota and PD, in that SCFAs could activate brain microglia cells to cause neuroinflammation and neuronal injury[3]. Misfolded α-synuclein in the small intestine was shown to spread into the brain along the vagus nerve, and severing the vagus nerve can prevent this transmission, suggesting a new intervention strategy for PD [8]. Study in the PTEN-induced kinase 1 (PINK1, a gene related to the human intestinal infection disease) knockout mice showed that intestinal infection acts as a triggering event in PD[9], which highlights the relevance of the gut-brain axis in this disease.

AD is a typical neurodegenerative disease. Although it was first described more than 100 years ago, its pathogenesis is still unclear. There are more than 30 hypotheses related to the occurrence and development of AD, including amyloid beta (Aβ) deposition, neurofibrillary tangles, neuroinflammation, and craniocerebral injury[4]. With rapid developments in life sciences, our understanding of the complex mechanism of AD pathogenesis has continuously expanded. Recently, it has been hypothesized that AD may be associated with dysbiosis of intestinal microbes, possibly via dysregulation of the P-glycoprotein pathway[10]. Another study of a Chinese cohort showed revealed distinct microbial communities like Gammaproteobacteria, Enterobacteriales, and Enterobacteriaceae are enriched in patients with AD [4]. Study have found that human herpes virus 6 a (HHV-6a) and 7 (HHV-7) are closely associated with AD and increase inflammatory cytokine levels in the brains of patients with neurodegenerative diseases[11]. Alteration of the gut microbiota can affect brain activity, which raises the possibility that therapeutic manipulation of the microbiome to treat AD and other neurological disorders[10]. Present studies and clinical trials indicate that there is an immense potential of gut microbiome modifications to be preventive or therapeutic[12]. We previously investigated the use of medicinal fungi as candidate compounds to treat AD and identified 3-hydroxyhericenone F as a promising, naturally occurring chemical constituent to treat AD by inhibiting β-secretase [13]. Alcohol extracts of *Ganoderma lucidum* are another promising, naturally occurring chemical constituent for the treatment of AD that regulates DNA methylation in D-galactose-induced deficient rats, and amyloid precursor protein (APP)/presenilin 1 (PS1) and senescence accelerated mouse-prone 8 (SAMP8) mice[14], *Bajijiasu* [15] and fructo-oligosaccharides from *Morinda officinalis* could also ameliorate AD in mice via improving the gut microbiota[16]. This field of research is currently undergoing great development, but contributions of many components of the gut-brain axis remain to be identified. Thus, more research is needed to delineate microbiome factors that may alleviate neurodegeneration. We must first understand how and when gut bacteria act to promote AD. The goal of this study was to establish the role of gut microbiota in AD, and to provide a basis for modifying gut microbiota with pre-, pro-, or antibiotics to treat AD. In this study, APP/PS1 mice were cohoused with pregnant mice until 1 week after birth, and the gut microbiota, learning and memory skills,

and metabolome were evaluated. We also compared the fecal microbes and metabolomes between healthy controls, disease controls, and AD patients.

Methods

AD patient feces sample collection

All participants or their legally authorized caregivers were informed of the purpose of this study, and all enrolled subjects provided written informed consent. The study was approved by the ethics committee of the fifth affiliated hospital, School of Medicine, Guangzhou Medical University, China. A total of 98 subjects (AD, n = 48; controls, n = 28) were recruited. The AD and control participants were aged 50–95 years. The control group was elderly people of a similar age to the AD group, who were in good health and did not suffer from major diseases. The healthy controls were 20–35 years old and in good health.

AD patients in this study were diagnosed according to both the criteria of the Diagnostic and Statistical Manual (DSM)-IV (Psychiatric Association. Committee on and Statistics, 1994) and guidelines of the National Institute of Neurological and Communicative Disorders and the Stroke and Alzheimer Disease and Related Disorders Association (NINCDS-ADRDA) [17], including early episodic memory impairment for > 6 months and the presence of medial temporal lobe atrophy. Participants with health or other diseases were also diagnosed according to appropriate ways in the hospital.

Patients with other causes of cognitive impairment were excluded from this study. We also excluded subjects who had a history of using antibiotics, probiotics, prebiotics, or synbiotics within 1 month before fecal sample collection; those with severe malnutrition, infection, or drug or alcohol dependence; irritable bowel syndrome; inflammatory bowel disease in the last year; and people with schizophrenia, schizoaffective disorder, or primary affective disorder; heart, brain, liver, kidney and hematopoietic system diseases or other serious primary diseases; and subjects with severe auditory, visual, or motor deficits that may interfere with cognitive testing.

AD cohousing mice

Adult C57 mice (16–20 g, 2 months, 20 female and 10 male), and Male APP/PS1 mice (7 months old, mean body weight 20 ± 5 g) were obtained from the Center of Laboratory Animals of Guangdong Province (SCXK [Yue] 2008-0020, SYXK [Yue] 2008-0085) and pair-housed in plastic cages in a temperature-controlled (25 ± 2 °C) colony room on a 12-/12-h light/dark cycle. Food and water were available ad libitum. All experimental protocols were approved by the Center of Laboratory Animals of the Guangdong Institute of Microbiology. All efforts were made to minimize the number of animals used. After 1 week of adaptive feeding, the C57 mice were fertilized by one male housed with two females, 2 weeks after pregnancy, fecal microbiota transplantation (cohousing) was performed.

By consulting the literature [8] and our preliminary research basis, we used the method of cohousing in a single cage. When mice had been pregnant for 2 weeks, two 8-month-old APP/PS1 mice per cage were

cohousing until 14 days after birth, when the APP/PS1 mice were removed. The control group was treated the same as the model group, but APP/PS1 mice were replaced with 8-month-old C57 mice.

Electrophysiological recordings

Standard field potential recordings were performed on the hippocampal cornu ammonis 1 (CA1) region using borosilicate glass micropipettes pulled to a tip diameter of about 1 μm and filled with 2 mol/L NaCl [18]. To record synaptic potentials, a recording electrode was placed at the CA1 apical dendrite region. Stimulus intensity was set based upon input-output relationships and was 50% of the maximal response. For testing paired pulse facilitation (PPF), two stimuli with 50% of the maximal intensity were given at 15-, 50-, 100-, and 400-ms intervals. For recording long-term potentiation (LTP), stable baseline synaptic potentials (50% of the maximal intensity) were recorded for 20 minutes, and then a theta-burst tetanic stimulation that contained 15 burst trains at 5 Hz was delivered (each train contained five pulses at 100 Hz). Thereafter, baseline intensity- evoked field excitatory postsynaptic potentials (fEPSPs) were recorded for 60 minutes with 0.33 Hz. A custom bipolar platinum wire electrode (0.08-mm diameter) was placed at the Schaffer collateral pathway, and stimulation was delivered using a Model 2100 A-M Systems Isolated Pulse Stimulator (Carlsborg, WA, USA). All evoked responses were recorded using an Axoclamp-2B amplifier, and data acquisition was controlled with pClamp 10.2 software (Molecular Devices, Sunnyvale, CA, USA).

Pathological and physiological examination

After the mice sacrificed, the brain and intestinal tissues were dissected. A total of four brains from each group were fixed in 4% paraformaldehyde solution and prepared as paraffin sections. Sections were stained with hematoxylin-eosin (H&E), and immunofluorescent assays were performed for ionized calcium-binding adaptor molecule 1 (IBA1) and glial fibrillary acidic protein (GFAP) using paraffin-embedded 3 μm sections and a two-step peroxidase-conjugated polymer technique (DAKO Envision kit, DAKO, Carpinteria, CA). Slides were observed by light microscopy[4] .

Microbiome analysis

Fresh intestinal content samples were collected before the fasting of mice and stored at -80 °C. Frozen microbial DNA isolated from these samples had total masses ranging from 1.2 to 20.0 ng and were stored at -20 °C. The microbial 16S rRNA genes were amplified using the forward primer 5'-ACTCCTACGGGAGGCAGCA-3' and the reverse primer 5'-GGACTA CHVGGGTWTCTAAT-3', and the forward primer 5'-CCTAYGGGRBGCASCAG-3' and reverse primer 5'-GGACTACNNGGGTATCTAAT-3' for mice. Each amplified product was concentrated via solid-phase reversible immobilization and quantified by electrophoresis using an Agilent 2100 Bioanalyzer (Agilent, Santa Clara, CA, USA). After quantification of DNA concentration by NanoDrop, each sample was diluted to a concentration of 1×10^9 molecules/μL in Tris-EDTA buffer solution and pooled. Next, 20 μL of the pooled mixture was used for sequencing with Illumina MiSeq sequencing system according to the manufacturer's instructions (Illumina, San Diego, CA, USA). The resulting reads were analyzed as described previously [19].

Metabolomic analysis

Mice feces

A 40 mg feces sample was homogenized in 400 µL deionized water containing 10 µg/mL of L-norvaline as internal standard. Following centrifugation at 14,000 g and 4 °C for 15 min, a total of 300 µL supernatant was transferred. The extraction was repeated by adding 600 µL of ice-cold methanol to the residue. The supernatants from the two extractions were combined. A 400 µL volume of combined supernatants and 10 µL of internal standard solution (50 µg/mL of L-norleucine) were combined and evaporated to dryness under nitrogen stream. The residue was reconstituted in 30 µL of 20 mg/mL methoxyamine hydrochloride in pyridine, and the resulting mixture was incubated at 37 °C for 90 min. A 30 µL volume of Bis(trimethylsilyl)- trifluoroacetamide (BSTFA) (with 1% trimethylchlorosilane (TMCS)) was added into the mixture and derivatized at 70 °C for 60 min prior to gas chromatography-mass spectrometry (GC-MS) metabolomics analysis.

Metabolomics instrumental analysis was performed on an Agilent 7890A gas chromatography system coupled to an Agilent 5975C inert MSD system. An OPTIMA® 5 MS Accent fused-silica capillary column (30 m × 0.25 mm × 0.25 µm; MACHEREY-NAGEL, Düren, Germany) was utilized to separate the derivatives. Helium (> 99.999%) was used as a carrier gas at a constant flow rate of 1 mL/min through the column. Injection volume was 1 µL in split mode (2:1), and the solvent delay time was 6 min. The initial oven temperature was held at 70 °C for 2 min, ramped to 160 °C at a rate of 6 °C/min, to 240 °C at a rate of 10 °C/min, to 300 °C at a rate of 20 °C/min, and finally held at 300 °C for 6 min. The temperatures of the injector, transfer line, and electron impact ion source were set to 250 °C, 260 °C, and 230 °C, respectively. The electron ionization energy was 70 eV, and data were collected in a full scan mode (m/z 50–600).

The typical total ion current chromatograms are illustrated in Figure S1. The peak picking, alignment, deconvolution, and further processing of raw GC-MS data were from previously published protocols[20]. The final data were exported as a peak table file, including observations (sample name), variables (rt_mz), and peak areas. The data were normalized against total peak abundances before performing univariate and multivariate statistics.

For multivariate statistical analysis, the normalized data were imported to SIMCA software (version 14.1, Umetrics, Umeå, Sweden), where the data were preprocessed with unit variance scaling and mean centering before performing principal component analysis (PCA), partial least squares discriminant analysis (PLS-DA), and orthogonal PLDS-DA (OPLS-DA). The model quality is described by the R^2X or R^2Y and Q^2 values. R^2X (PCA) or R^2Y (PLS-DA and OPLS-DA) is defined as the proportion of data variance explained by the models and indicates the goodness of fit. Q^2 is defined as the proportion of variance in the data predictable by the model and indicates the predictability of current model, calculated by a cross-validation procedure. To avoid model over-fitting, we performed a default 7-round cross-validation in SIMCA software to determine the optimal number of principal components.

For univariate statistical analysis, the normalized data were analyzed on the R platform (version 3.3.0). Parametric testing was performed on normally distributed data by Welch's *t* test, while nonparametric Wilcoxon Mann-Whitney tests were conducted on the data with abnormal distributions.

The variables with VIP values in the OPLS-DA model > 1 and p values for univariate statistical analysis < 0.05 were identified as potential differential metabolites (Fig. 8B). Fold change was calculated as a binary logarithm of the average normalized peak intensity ratio between Groups 1 and 2, where a positive value means that the average mass response of Group 1was higher than Group 2.

Mice serum

Serum was collected after the mice were sacrificed, and 80 μL serum was added into 240 μL of cold methanol with acetonitrile (2:1, v/v). Next, 10 μL internal tagging standard (L-2-chlorine-phenylalanine, 0.3 mg/mL, dissolved in methanol) was added, vortexed after 2 min, then extracted using ultrasonic extraction method for 5 min. After 20 min standing at -20 °C and centrifuging for 10 min (14000 prm, 4 °C), 200 μL of supernatant was loaded into a sample bottle with lining tube for liquid chromatography-mass spectrometry (LC-MS) analysis (Waters UPLC I-class system equipped with a binary solvent delivery manager and a sample manager, coupled with a Waters VION IMS Q-TOF Mass Spectrometer equipped with an electrospray interface (Waters Corporation, Milford, MA, USA). LC Conditions: Column: Acquity BEH C18 column (100 mm × 2.1 mm i.d., 1.7 μm; Waters). Data analysis was performed as described previously for feces experiments.

RNA sequencing

We prepared RNA sequencing libraries using global brain samples and performed 150-bp paired-end sequencing using the Illumina HiSeq platform. RNA sequencing libraries were prepared from 2 μg of total RNA using the TruSeq Kit (Illumina) with the following modification: instead of purifying poly-A RNA using poly-dT primer beads, we removed ribosomal RNA using the Ribo-Zero rRNA Removal Kit (Illumina). All other steps were performed according to the manufacturer's protocols. RNAseq libraries were analyzed for quality control, and the average size of inserts was approximately 200 to 300 bp. The sequencing library was then sequenced on a Hiseq platform (Illumina).

Western blotting analysis

Cells were seeded into 6-well culture plates at 5×10^6 cells/well and washed twice with D-Hanks solution when the cells reached 80% confluence. The cells were harvested and lysed with protein lysis buffer, and protein concentrations were determined using a Coomassie Brilliant Blue G250 assay kit (Nanjing JianCheng Bioengineering Institute, Nanjing, China).

The brain tissue was also assessed. Briefly, brain tissue was dissected from AD-cohousing treated mice (purchased from Beijing HFK Bioscience Co., LTD [Certificate No: SCXK (Jing) 2014-0004]) and proteins were extracted with radioimmunoprecipitation assay lysis buffer (T-PER™ Tissue Protein Extraction Reagent, 78510; Thermo Fisher Scientific, Waltham, MA, USA). The proteins were separated by sodium dodecyl sulfate-polyacrylamide gel electrophoresis and transferred onto polyvinylidene fluoride

membranes. After blocking with 5% nonfat dry milk in Tris-buffered saline (20 mM Tris-HCl, 500 mM NaCl, pH 7.4) with 0.2% Tween-20 (T104863; Aladdin, Shanghai, China), the membranes were probed with antibodies overnight at 4 °C, followed by incubation with a horseradish peroxidase-conjugated goat anti-mouse (G2211-1-A; Servicebio, Wuhan, China) or goat anti-rabbit (G2210-2-A, Servicebio) IgG secondary antibody (1:2000).

The antibodies were as follows; IBA-1 (10904-1-AP; Proteintech, Rosemont, IL, USA), GFAP (20746-1-AP, Proteintech), p-Tau (Ser416, AF2420), p-Tau (Ser717/400, AF8129), p-Tau (Ser262, AF3151), p-Tau (Ser235, AF3142), p-Tau (Ser356, AF3143), p-Tau (Ser202, AF2419), p-Tau (Ser199, AF2418), p-Tau (Ser396, AF3148), p-Tau (Ser214, AF3141), p-Tau (Ser404, AF3144), p-Tau (Ser422, AF3145), p-Tau (Thr498/181, AF3149), p-Tau (Thr212, AF3146), p-Tau (Thr231, AF3147), p-Tau (Thr205, AF3150), CD33 (#AB32577; AbSci, Vancouver, WA, USA), TREM2 (ab86491; Abcam, Cambridge, UK), interleukin (IL) 12α (AF5133), PYCARD (DF6304), PI3Kp85 (60225-1-AP, Proteintech), PI3Kp100 (60224-1-AP, Proteintech), AMPK (80039, Abcam), p53 (66064, Abcam), Atg13, Atg14 (19491-1-AP, Proteintech), Atg5 (10458-1-AP, Proteintech), Atg12 (1825-1-AP, Proteintech), LC3A/B (128025, Abcam) were obtained from Affinity as well as GAPDH (2118L; Cell Signaling Technologies [CST], Danvers, MA, USA) and β-actin (4970S, CST). Band intensity was quantified using ImageJ software (National Institutes of Health, Bethesda, MD, USA).

Statistical analysis

All data are means ± standard deviations (SD) of at least three independent experiments. Significant differences between treatments were analyzed by one-way analysis of variance at $p < 0.05$ using Statistical Package for the Social Sciences (SPSS, Chicago, IL, USA) and Prism 5 (GraphPad, San Diego, CA, USA) software.

Results

Variation characteristics of gut microbiota in AD patients

Following ethics committee approval, feces was collected from 47 AD patients, 28 disease controls, and 26 healthy controls. The 16S rRNA analysis showed significant differences for the abundance-based covered estimator (ACE) and Chao 1 indexes ($p < 0.05$, Fig. 1A) from the healthy groups. The heatmap of genus abundance and the relative abundance of changed bacteria of the AD group show that the genera, *Faecalibacterium*, *Fusicatenibacter*, *Roseburia*, *Lachnospira*, *Agathobacter, Megamonas* and *Prevotella 9* were decreased, while *Klebsiella*, *Akkermansia*, *Rhodococcus*, *Pseudomonas and Escherichia-Shigella* were increase compared to the healthy group(Fig. 1B). The three-phase diagram (Fig. 1C) showed that the abundances of some of bacteria species varied, with higher levels of conditioned pathogens in the disease groups, suggesting these bacteria may indicate an AD-related gut microbiota. To evaluate the role of gut microbiota on AD pathogenesis, we performed cohousing in mice.

The gut microbiota composition of normal C57 mice and APP/PS1 mice

Before couhousing, we analyzed the gut microbiota composition of APP/PS1 mice using 16S rRNA sequencing. As shown in Fig. 2, the heatmap at genus (Fig. 2A) levels could successfully distinguish the normal 8-month C57 and 8-month APP/PS1 mice. The relative abundances of *Alistipes*, *Rikenella*. *Anaerotruncus*, *Turicibacter*, *Mucispirillum*, *Adlercreutzia*, *Desulfovibrio*, *Lactobacillus* were increased compared to control, while *Ruminococcus*, *Oscillospira* and *Clostridium*, *Prevotella*, *Sutterella*, *Anaerostipes* and *Bacillus* were decreased (Fig. 2A, $p < 0.05$). The results revealed that the gut microbiota composition of APP/PS1 mice were very different from the normal C57 mice.

Colonization of gut microbiota analysis

To explore the role of gut microbiota on AD pathogenesis, an cohousing model was used. After consulting the literature and considered our preliminary results, we used the methods of cohousing. after 2 weeks of pregnancy, the dams were placed with two 8-month-old APP/PS1. The mice were cohoused until 14 days after birth.

At first and second time points, the gut microbiota composition of intestinal contents were analyzed. For the offspring of mice fed a standard diet, as shown in Fig. 3A, the operational taxonomic units (OTUs) of AD-cohousing mice (287 of S1N, 328 of S2N) were lower than that of control groups (318 of Control 1, 357 of Control 2). The heatmap of the relative abundance of genus showed obvious variation after cohousing with APP/PS1 mice (Fig. 3B). The ACE, Chao 1 and Shannon indexes showed the same trends, while groups S1N and S2N were lower than their corresponding control groups (S1N vs Control 1, S2N vs Control 2). Collectively, these results indicate that some bacteria could be colonized from APP/PS1 mice to newborn C57 mice during cohousing.

The dominant bacterial communities were the Firmicutes and Bacteroidetes (Figure S1). The main differences in bacteria abundance at genus levels were decreases in *uncultured bacterium Bacteroidales S24-7 group, Desulfovibrio, Turicibacter, Candidatus Saccharimonas*, while *Lactobacillus*, *Ruminiclostridium 5*, *Odoribacter*, *uncultured bacterium Porphyromonadaceae* were increase (Fig. 3B, S1N vs Control 1, $p < 0.05$). The main differences in bacteria abundance at genus levels were decreases in *Enterorhabdus*, *Ruminiclostridium*, *Desulfovibrio*, *Alloprevotella*, *uncultured bacterium Ruminococcaceae*, while *uncultured bacterium Mollicutes RF9*, *Lactobacillus*, *Candidatus Saccharimonas*, *Turicibacter* and *Ruminococcaceae UCG-014* were increased (Fig. 3B, S2N vs Control 2, $p < 0.05$).Those suggests that cohousing with APP/PS1 mice expands the differentiation of gut microbiota, or the bacteria from APP/PS1 mice could affect the microbe colonization that the normal C57 mice received from their mothers. A PCoA plot also show the different between S1N group and control1 group and between S2N group and control2 group(Figure S2). *Lactobacillus* and *Turicibacter* was increased both in cohousing mice and 8-month APP/SP1 mice, which may be the dominant species of colonization.

LTP (Long-term Potentiation) in hippocampal slices

Based on the colocalization of gut microbiota analysis using 16S rRNA, the mice were kept on their diets for 10 months, based on the fact APP/PS1 mice begin to exhibit learning and memory dysfunction at 6 months old[21]. Ten months later, subsets of mice were randomly selected to perform standard field

potential recordings. Repetitive stimulation (0.33 Hz) of Schaffer collaterals evoked fEPSPs in the hippocampal CA1 region (Figs. 4A, $p < 0.05$). The input-output relationship curves (Figs. 4B, $p < 0.05$) and linear slopes (4C, $p < 0.05$) revealed that compared to control mice (NC), the hippocampal CA1 neurons of cohousing mice showed decreased excitability. Synaptic short-term plasticity was measured using a PPF protocol in hippocampal slices. Statistical analyses from all slices demonstrated a significant inhibition of the ratio of P2/P1 at all tested P1 and P2 intervals in AD-cohousing mice compared to control mice of NC (Figs. 4D, $p < 0.05$), suggesting decreased hippocampal synaptic short-term plasticity. Finally, hippocampal CA1 synaptic LTP between AD-cohousing and control mice were compared. The plot recording time to normalized fEPSP slopes (baseline as 1) from pooled data showed impaired LTP induction (after theta-burst stimulation 0–10 min) and maintenance (after theta-burst stimulation 50–60 min) (Figs. 4E, $p < 0.05$, unpaired *t* test). The mean LTP induction results are shown in Figs. 4F and Figs. 4G ($p < 0.05$, unpaired *t* test).All these results suggested that reduced LTP occurs in AD-cohousing mouse hippocampus.

AD-cohousing enhances inflammation in brain and serum

Based on the gut microbiota structure changes and altered LTP in hippocampal slices after cohousing, we assessed brain morphology in mice. The remaining mice were sacrificed, and the brain sections were processed for H&E and Nissl staining, which showed obvious pathologic changes as the neuron shrinkage, neuron size and number reductions, and cytoplasmic vacuolar changes in AD-cohousing mice. Immunofluorescent labeling of microglial IBA-1 and GFAP in the CA1 area showed strong astrocyte and microglial activation (Fig. 5A).

Next we measured serum levels of the cytokines tumor necrosis factor-alpha (TNF-α), epidermal growth factor (EGF), IL-17α, prolactin, fibroblast growth factor (FGF)-basic, monocyte chemoattractant protein (MCP)-1, IL-6, granulocyte colony-stimulating factor (G-CSF), and macrophage inflammatory protein (MIP)-1α. The results shown in Fig. 5B show that MIP-1α was changed significant after AD-cohousing, which indicated that bacteria from the APP/PS1 mice could colonize the intestines of newborn mice and influence their inflammatory reactions.

AD-cohousing accelerates Tau protein hyperphosphorylation, inflammation and autophagy.

To clarify the action of cohousing on AD pathogenesis, we first assessed the AD biomarkers of Tau, Aβ4, β-site APP cleaving enzyme (BACE), and apolipoprotein E (APOE) in the brain. Their expression levels shifted after cohousing. Tau, Aβ4, BACE, and APOE were upregulated in most AD-cohousing mice($p < 0.05$, Fig. 7A and Fig. 8A).

Abnormal hyperphosphorylation of Tau is positively correlated with cognitive dysfunction, neurofibrillary degeneration and the degree of dementia [22]. we further detected the different phosphorylation sites of Tau protein using specific antibodies. The difference was significant for p-Tau(Ser404) and p-Tau(Ser416) ($p < 0.05$, Fig. 7A), which indicated enhanced Tau protein hyperphosphorylation.These

results indicate that AD gut microbiota could accelerate Tau protein hyperphosphorylation on multiple sites.

The inflammatory factors of TREM2, IL-12α, IL-23, NF-κB p65, NLRP3 and TLR4; the oxidative stress biomarker GSK3β and autophagy biomarkers of LC3A/B, Atg14, AKT, Atg12, and PI3K p85 in AD-cohousing mice brain tissue provided reliable evidence that AD fecal metabolites or bacteria can induce autophagy, inflammation, oxidative stress, and Tau protein hyperphosphorylation(Fig. 6A and Fig. 7A). In other words, AD gut microbiota can accelerate Tau protein hyperphosphorylation crosstalk that involves both inflammation and autophagy.

Fecal metabolites induce inflammation and autophagy in BV2 cells

To investigate the factors related to Tau protein hyperphosphorylation, we co-cultured BV2 cells with AD-cohousing mice feces extracts. Then we performed western blotting to measure the oxidative stress biomarker glycogen synthase kinase 3 (GSK3)β, the inflammatory factor of nuclear factor (NF)-κB, the autophagy biomarkers of microtubule-associated protein light chain (LC)3A/B, and levels of Tau and p-Tau using western blotting. The results (Fig. 8A) showed that autophagy, inflammation, and oxidative stress were influenced by the extracts of AD-like mice feces, which indicated that AD fecal metabolites can induce an imbalance of autophagy and activate inflammation and oxidative stress in BV2 cells.

PKA, PGLYRP2 and NOX1 (Fig. 8A) levels were altered by extracts of AD-cohousing mice feces (17.25 mg/ml high dose, AD-cohousing-H; 13.5 mg/ml of middle dose, AD-cohousing-M; and 7.7 mg/ml low dose, AD-cohousing-L; 13.5 mg/ml of middle dose, Control), which indicated GSK3β/protein kinase A (PKA) activation, which can lead to an imbalance in reactive oxygen species (ROS) and then aggravate oxidative damage and/or aging.

Metabolomics analysis of intestinal contents and serum in AD- cohousing mice

Based on the effects of extracts of AD-cohousing mice feces on BV2 cells, we performed metabolomics analysis of intestinal contents to investigate the target bacteria and/or metabolites. The metabolomics of intestinal contents were analysis using GC-MS, and serum was assessed with LC-MS. As shown in Fig. 8 and Fig. 9 .

19 metabolites were identified *in fimo* (Fig. 8B) and 58 metabolites (Fig. 9A) that significantly distinguished control and AD-cohousing mice. There were higher levels of glucose, maltose, lactic acid, sorbitol, and ribose in feces of AD-cohousing mice compared to control, which indicated that the glycometabolism are abnormal. The AD-cohousing mice also had higher serum levels of bucillamine, 3,4-dihydroxyphenylpropionic acid, hippuric acid, acetyl-methylcholine, pregabalin, methionine, cinnamic acid, DL-phenylalanine, L-(-)-methionine, 3-methylsulfolene, uric acid, L-(+)-citrulline, benzenesulfonamide, L-norleucine, valine, pyrrolidine, 2-hydroxy-2-methylbutyric acid, linoleic acid and oxibendazole (Fig. 9A).

Previous study have demonstrated that the leucine can activate the mTOR to regulate the autophagy and mitochondrial function [23]. In this study, we also found that the levels of leucine in feces were reduced, while norleucine levels were increased in serum, expressions of mTOR, TORC1 (CRTC1) and TORC2 (CRTC1) were up-regulated (Fig. 7A, $p < 0.05$). The difference of metabolism of feces and serum suggested that AD- cohousing disorder the leucine metabolism, make the mTOR unregulating the autophagy, then aggravates accumulation of pathological products and inflammation levels, but these still need more studies and clinical survey to confirm. Metabolites pathway analysis of differences metabolites of feces and serum between AD- cohousing mice and control in table 2 and table 3.

Discussion

Oxidative stress, inflammation, neurogenesis, immune responses, dysbacteriosis and infection all about above 30 factors have been associated with AD [24]. Gut microbiota can release significant amounts of harmful metabolites as amyloids and lipopolysaccharides, which might modulate signaling pathways and induce the production of proinflammatory cytokines related to AD pathogenesis. The gut microbiome, leaky gut, and bacterial translocation could be involved in AD. In this study, we also found evidence of dysbacteriosis in both AD patients and APP/PS1 mice (Figs. 1–3), especially an increase in pathogenic and conditioned pathogens in AD patients (Fig. 1). The behavior, oxidative stress, inflammation, neurogenesis, and immune response of AD-cohousing mice were altered compared to normal control mice (Figs. 3–7). However, some of them are beneficial or exert different functions dependent on the numbers of other bacteria, as members of the *Alistipes* genera show high abundance in the most frail individuals and in middle-aged and older mice and are decreased in autism spectrum disorders, colitis and colorectal cancer, chronic hepatitis B patients, and appendicitis [1, 25]. Several studies reported that *Bacteroides fragilis* (*B. fragilis*), members of *Bacteroides*, and its immunomodulatory capsular polysaccharide A are equally effective in preventing colitis and experimental allergic encephalomyelitis in murine models [26]. These species also orchestrate robust protective anti-inflammatory responses during viral infections [22]. Rodents with high abundance of *Alloprevotella* genera in early life have high risk of behavioral phenotypes, with males but not females exhibiting deficits in social behavior [27]. Clinical investigation showed that the genera *Lactobacillus*, *Clostridium IV*, *Paraprevotella*, *Clostridium sensu stricto*, *Desulfovibrio*, and *Alloprevotella* were enriched in fecal samples from patients with chronic kidney disease [28].

Serum levels of many cytokines (TNF-α, EGF, IL-17α, prolactin, FGF-basic, MCP-1, IL-6, G-CSF, and MIP-1α) measured after cohousing (Fig. 5), and brain levels of inflammatory factors were also altered, including TREM2, IL-12α, IL-23, NF-κB p65, NLRP3 and TLP4 (Fig. 6 and Fig. 7). Extracts of AD-cohousing mice feces influenced levels of GSK3β, NF-κB, and LC3A/B in BV2 cells. Collectively, the results shows that gut microbiota change modulate signaling pathways and the production of proinflammatory cytokines related to AD pathogenesis. Although these limited microbiota animal models do not fully represent the situation in humans, there is considerable evidence of a role of gut microbiota in AD progression.

Recent human studies have investigated gut bacterial taxa and shown altered abundance in patients with AD [29]. A Chinese cohort had distinct microbial communities of *Gammaproteobacteri*a, *Enterobacteriales*, and *Enterobacteriaceae*[4]. Li *et al*. studied AD patients and found that the fecal abundance of six genera increased (*Dorea*, *Lactobacillus*, *Streptococcus*, *Bifidobacterium*, *Blautia*, and *Escherichia*), while five decreased (*Alistipes*, *Bacteroides*, *Parabacteroides*, *Sutterella*, and *Paraprevotella*) [28]. They also found that blood samples had different abundances between control and AD groups; *Propionibacterium*, *Pseudomonas*, *Glutamicibacter*, *Escherichia*, and *Acidovora* increased, while *Acinetobacter*, *Aliihoeflea*, *Halomonas*, *Pannonibacter*, *Leucobacter*, and *Ochrobactrum* decreased [28]. We found that the genera of *Megamonas, Faecalibacterium,Lachnospira, Fusicatenibacter*、*Prevotella 9* and *Ruminococcus_2* were decreased, *while Rhodococcus* were increase compared to the control group (Fig. 1B). The commonly changed bacteria in AD-like mice and AD patients only belonged to the *Lactobacillus* genera, the more pathogenic bacteria in the AD patients were not found in specific pathogen-free (SPF) AD-like mice, and few special bacteria found were different from previous studies[4, 28, 29]. *L. plantarum*-derived lactic acid triggered the activation of the intestinal NADPH oxidase Nox and ROS generation. In turn, ROS production promoted intestinal damage, increased intestinal stem cell proliferation, and dysplasia. Nox-mediated ROS production required lactate oxidation by the host intestinal lactate dehydrogenase, revealing host-commensal metabolic crosstalk that is probably broadly conserved [3]. The increase in intestinal permeability coincided with higher plasma levels of LPS, serum IL-1, and TNF-α. Clinical studies suggested that individuals with microbial dysbiosis due to intestinal diseases have a higher risk of AD [28]. In this study, the fecal metabolites of AD-cohousing mice influenced PGRP-L and NOX1 expression in BV2 cells (Fig. 8A). Systemic inflammation was also observed. The study reveals marked sex differences in a multifactorial model of early-life adversity, both on emotional behaviors and gut microbiota and *Lactobacillus* genera was regulated by early adversity both in male and female[27]. Previous studies suggest that gut microbiota is associated with neuropsychiatric disorders, such as Parkinson'disease, amyotrophic lateral sclerosis, and depression. In the present study, clinical fecal samples were collected and analysed from AD patients for 16S ,which show gut microbiota is altered in AD patients and may be involved in the pathogenesis of AD[29].

Major group of microbes linked to AD include bacteria: *Chlamydia pneumoniae*, *Helicobacter pylori*, *Porphyromonas gingivalis*, *Fusobacterium nucleatum*, *Prevotella intermedia*, *Actinomyces naeslundii*, and spirochete group; fungi: *Candida sp*., *Cryptococcus sp*., *Saccharomyces sp*., *Malassezia sp*., *Botrytis sp*., and viruses: herpes simplex virus type 1 (HSV-1), human cytomegalovirus, and hepatitis C virus [10]. We also found that the pathogenic bacteria including *Escherichia*, *Klebsiella*, *Pseudomonas*, *Rhodococcus*, and *Akkermansia* were increased in AD patients, which indicated that these infections might an inducers and/or accelerators for oxidative stress, inflammation, autophagy, and neurodegeneration. *Escherichia* was increased at the genus level in both fecal and blood samples from subjects with AD and MCI [28]. Postmortem brain tissue from patients with AD showed that both LPS and gram-negative *Escherichia coli* fragments colocalize with amyloid plaques, and an increase in the abundance of a pro-inflammatory gut microbiota of *Escherichia-Shigella* and a reduction in anti-inflammatory *Eubacterium rectale* are possibly associated with a peripheral inflammatory state in patients with cognitive impairment and brain

amyloidosis [10, 28, 30]. In this study, we found a higher abundance of *Escherichia - Shigella* in AD patients, and the expressions of GSK3β, NF-κB, LC3A/B, Tau, and p-Tau correlated with metabolites of feces of AD-cohousing mice in BV2 cells. IgG antibody levels to seven oral bacteria associated with periodontitis showed that abundance of *Fusobacterium nucleatum* and *Prevotella intermedia* were significantly increased at baseline serum draw in the AD patients compared to controls, and these remained significant when controlling for baseline age, Mini-Mental State Exam score, and *APOE ε*4 status, which suggested that chronic inflammation in periodontal disease could be a risk factor for AD [10, 28, 30]. *F. nucleatum* is an anaerobic oral commensal and a periodontal pathogen associated with a wide spectrum of human diseases. It is implicated in adverse pregnancy outcomes (chorioamnionitis, preterm birth, stillbirth, neonatal sepsis, preeclampsia), gastrointestinal disorders (colorectal cancer, inflammatory bowel disease, appendicitis), cardiovascular disease, rheumatoid arthritis, respiratory tract infections, Lemierre's syndrome, and AD [10, 28, 30]. Subtractive genomics analysis demonstrated that *F. nucleatum* infection could simultaneously regulate multiple signaling cascades that could upregulate proinflammatory responses, oncogenes, modulation of host immune defense mechanisms, and suppression of DNA repair system [28]. Microcin E492, a peptide naturally produced by *Klebsiella pneumonia*, assembles into amyloid-like fibrils *in vitro*, and these have the same structural, morphological, tinctorial, and biochemical properties as the aggregates observed in AD [10, 28, 30]. Low levels of the amino acid L-arginine in astrocytes surrounding amyloid plaques may be observed because arginine deiminase from *Pseudomonas aeruginosa* and peptidylarginine deiminase from bovine brain are inhibited by amyloid peptides that contain arginine (amyloid 1–42), and enhanced peptidylarginine deiminase activity is noted with free L-arginine [4, 10, 28]. Most bacteria in AD patients were not found in SPF model mice, strongly suggesting that studies of gut microbiota in aseptic mice do not tell the full story. Investigations in wild gut microbiota mice and long-term clinical studies are urgently needed to determine if these bacterial alterations are a cause or effect of AD. A recently report ensured that the important role of microglia and NLRP3 inflammasome activation in the pathogenesis of tauopathies and support the amyloid-cascade hypothesis in Alzheimer’s disease, and demonstrated that neurofibrillary tangles develop downstream of amyloid-beta- induced microglial activation [4, 10, 28], and NLRP3 is considered as an intracellular sensor that senses multiple microbial antigens and endogenous danger signals[30, 31]. In this study, serum levels of the cytokines MIP-1α was altered after cohousing(Fig. 5B). There were also changes in brain levels of inflammatory factors including, TREM2, IL-12α, IL-23, NF-κB p65, NLRP3and TLP4, (Fig. 6 and Fig. 7). The AD biomarkers Amyloid-β-A4, Tau, p-Tau, and APOE were upregulated. So, we sure that the gut microbiota appear to play an indispensable role in modulating the gut-brain axis and could be an important pathogenic factor of AD, and target on the microbiome-gut-brain axis will be an effective action. However, it is not clear if this is a useful diagnostic biomarkers as the AD gut microbiota could be distinguished from the healthy group but not the disease control groups, it perhaps due to the small sample size.

Tau hyperphosphorylation is associated with abnormal Aβ aggregation in AD, there are specific temporal patterns of phosphorylated Tau in different parts of the brain [4, 10]. Tau hyperphosphorylation plays a vital role in regulating synaptic function and maintaining cytoskeletal integrity [4, 10, 28, 30]. In this study,

phosphorylation at sites Ser404 and Ser416 were upregulated after cohousing, indicating that the AD gut microbiota enhances Tau protein hyperphosphorylation at multiple sites. There are many factors regulating Tau phosphorylation level, including oxidative stress, inflammation, neurogenesis, immune response, dysbacteriosis, infection and autophagy dysfunction. Tau phosphorylation is also affected by oxidative stress, endoplasmic reticulum protein folding dysfunction, and protein clearance ability decreases mediated by the proteasome and autophagy [4, 10, 28, 30]. Normally, this abundant soluble protein can promote microtubule assembly and stability in axons, but this balance is upset when the Tau protein is hyperphosphorylated due to infection, metabolic disease, or chronic inflammation. Tau will be hyperphosphorylated and/or depolymerized depending on the activities of GSK-3β and the cell cycle protein-dependent kinase p25 [4, 10, 28]. As in Fig. 8A, the expression of GSK-3β was upregulated by AD feces extracts, and the autophagy was dysfunction.

Autophagy is a critical cellular process of internal degradation and recycling harmful or damaged components[31]. Autophagy dysfunction and tissue inflammation make people more susceptible to diseases, especially to intestinal diseases[32]. As a conservative serine/threonine protein kinase, mTOR is the junction of upstream pathways to regulate the cell growth, proliferation, movement, survival and autophagy [33], mTORC1 promotes the cell growth and metabolism, and inhibits autophagy by binding ULK1 complex [33]; and previous study have demonstrated that the leucine can activate the mTOR to regulate the autophagy and mitochondrial function [23]. In this study, we found that the levels of leucine in feces were reduced, while norleucine levels were increased in serum, expressions of mTOR and TORC1 were up-regulated in cohousing mice (Fig. 7A), and autophagy dysfunction (Fig. 7A), which indicate that AD-cohousing disorder the leucine metabolism, activate the mTOR to unregulated the autophagy. Dysfunction of autophagy aggravates the accumulation of pathological products and inflammation levels (Figs. 6–7). Moreover, systemic inflammatory reactions caused by compounds secreted by bacteria promote oxidative stress, neuroinflammation, autophagy and/or neurodegeneration as demonstrated in previous studies [28]. So, we conclude that harmful microbes and/or their metabolites from APP/PS1 mice implanted in the newborn mice, caused metabolic imbalance, activated chronic inflammatory responses and affected autophagy and tau protein hyperphosphorylation (cover). Therefore, targeting the gut microbiota could be an effective treatment to slow AD progression. The role of the complex gut microbiota in AD still requires further investigation both at the community and/or strain level.

Multivariable-adjusted analyses showed that sphingomyelins and ether-containing phosphatidylcholines were altered in preclinical biomarker-defined AD stages, whereas acylcarnitines and several amines, including the branched-chain amino acid valine and α-aminoadipic acid, changed in symptomatic stages [4, 10, 28, 30, 34]. Decreased neuronal glucose metabolism that occurs in AD brain could play a central role in disease progression [4, 10, 28, 30, 34]. And more evidences showed that amino acid oxidation can temporarily compensate for the decreased glucose metabolism, but eventually altered amino acid and amino acid catabolite levels likely lead to toxicities contributing to AD progression. Because amino acids are involved in so many cellular metabolic and signaling pathways, the effects of altered amino acid metabolism in AD brain are far-reaching [4, 10, 28, 30, 34]. In this study, we found that amino acid metabolism and lipid metabolism were imbalanced (Fig. 9, table S3), and we demonstrated that the

leucine metabolism imbalance induced the autophagy dysfunction, which aggravates the accumulation of pathological products and inflammation levels, these also indicated that regulate the metabolism balance targeting on the gut-brain axis is important for AD prevention and treatment.

Dietary, microbial, and inflammatory factors modulate the gut-brain axis and influence physiological processes ranging from metabolism to cognition [35]. Nutrients affect gut microbiota composition and the formation and aggregation of cerebral Aβ [35]. In a transgenic AD mouse model, AD pathology shifted gut microbiota composition toward an inflammation-related bacterial profile, suggesting that these changes could contribute to disease progression and severity [7]. The gut microbiota has been shown to mediate the anti-epileptic effect of a ketogenic diet [7, 35]. Metabolites of dietary tryptophan produced by microflora control microglial activation, affect TGFα and vascular endothelial growth factor-β production, regulate transcription in astrocytes, and modulate CNS inflammation via the aryl hydrocarbon receptor, with implications for anxiety and depression [36]. The diet also impacts AD progression; germ-free mice demonstrated deficits in nonspatial and working memory tasks, as well as reduced hippocampal expression of brain-derived neurotrophic factor[37]. Uridine- and docosahexaenoic acid-containing diets could prevent rotenone-induced motor and gastrointestinal abnormalities associated with the pathogenesis of PD[37]. Altered gut microbiota composition has been associated with the onset of AD, which is characterized by the cerebral accumulation of amyloid-β fibrils[37]. It is therefore possible that modulation of the gut microbiome by specific nutritional intervention may prove to be an effective strategy to prevent or reduce the risk of neurodegenerative disorders, such as PD and AD.

Conclusions

The gut microbiota structure of AD patients are different from control groups, which suggest that there is a certain correlation between gut microbiota and AD. Special pathogenic bacteria were found in AD patient samples, which might induce and/or accelerate disease processes. Gut microbiota from APP/SP1 mice changed structure of gut microbiota of newborn mice. The effect of changes in gut microbiota structure in cohousing mice, which may cause the leucine metabolism disorder and induces the mTOR mediates autophagic dysfunction, then aggravates inflammation levels and Tau protein phosphorylation. Subsidiary experiments in BV2 cells shows the same trends. These findings indicate that the metabolites of gut microbiota may induce and/or accelerate autophagy, inflammation, and neurodegeneration and participates in the process of AD by accelerating Tau protein phosphorylation.

Study Limitations

There are several strengths of this study, but there are also limitations. For example, we couldn’t figure out which bacterial specie is associated with AD, or maybe many microorganisms with the whole action. And we have not perform a rescue test with single bacteria species, so we could not confirm direct contact between p-Tau and single bacteria, and we could not determine the specific signaling pathway. Fecal transplants of targeted strains in germ-free mice with multi-omics studies will clarify interactions in the microbiome-gut-brain axis, and experiments in genetically altered mice could provide further evidence

supporting our hypothesis. And long-term clinical monitoring are needed to screen dietary and nutritional interventions for AD based on gut microbiota.

Declarations

Ethical Approval and Consent to participate

The animal protocols used in this work were approved by the Institutional Animal Care and Use committee of the Center of Laboratory Animals of the Guangdong Institute of Microbiology.

Consent for publication

Not applicable.

Availability of data and materials

Data collection and sharing for this project was funded by the National Natural Science Foundation of China.

Competing interests

The authors declare that they have no competing interests.

Funding

The present work was supported by the financial support from the National Natural Science Foundation of China (81701086)

Authors’ contributions

Chen DL and Wang Jian designed the study, carried out the computational analyses and wrote the manuscript; Guo YR, Qi LK and Tang XC collected animal physiological data and fecal samples and extracted ruminal DNA. Guo YR, Qi LK, Liu YD and Zeng M collected the Metabolomic analysis results; Yang X, Zhu XX, Deng TM, Wang DD and Fu YH collected AD patient samples. Li R collected the animal LTP data; Chen DL, Guo YR, Liu YD, Zhu XX, and Zeng M collected data regarding the pathological test, microbial metabolic networks and transcriptome analysis. Tang XC, Guo YR, Liu YD and Zeng M collected animal WB data. Xie YZ, Wang Jian and Chen DL helped to design the study and to develop the metagenomic analysis tools and reviewed the manuscript. All authors read and approved the final manuscript.

Acknowledgments

We would like to thank Zhang Maolei for helpful discussions in the preparation of this manuscript. Sequencing services were provided by Biomarker Technologies Co., Ltd. Beijing, China, and Guangzhou Geneseed Biotech Co.,Ltd. Guangzhou, China.

Author details

[1]School of Basic Medical Science, Guangzhou University of Chinese Medicine, Guangzhou510000, China

[2]State Key Laboratory of Applied Microbiology Southern China; Guangdong Provincial Key Laboratory of Microbial Culture Collection and Application; Guangdong Open Laboratory of Applied Microbiology; Guangdong Institute of Microbiology, Guangdong Academy of Sciences, Guangzhou China 510070

[3]The Fifth Affiliated Hospital of Guangzhou Medical University, Guangzhou 510700, China

[4]Department of Physiology, Shantou University Medical College, Shantou 515063, China

[5]Academy of Life Sciences, Jinan University, Guangdong Province, Guangzhou 510000, China

[6]Chengdu University of Traditional Chinese Medicine, Chengdu 610075, Sichuan, China

[7]Deparment of Intensive Care Unit, Guangzhou First People's Hospital; School of Medicine, South China University of Technology, Guangzhou 510000, Guangdong, China

Guo Yinrui (75706868@qq.com); Tang Xiaocui (107236594@qq.com);Qi Longkai (qi371605700@qq.com); Yang Xin (chemist_yx@163.com); Li Ran (610087390@qq.com); Zhu Xiangxiang (2859281601@qq.com); Zeng Miao (1220799848@qq.com); Deng Tianming (dtm211619@163.com); Fu Yonghong (2089919@qq.com); Xie Yizhen (xieyzihen@126.com); Wang Jian (zswj@gzucm.edu.cn); Chen Diling (diling1983@163.com)

References

1. Strati F, Cavalieri D, Albanese D, De Felice C, Donati C, Hayek J, Jousson O, Leoncini S, Renzi D, Calabrò A, et al: **New evidences on the altered gut microbiota in autism spectrum disorders**. *MICROBIOME* 2017, 5(1).
2. Lach G, Lach G, Schellekens H, Schellekens H, Dinan TG, Dinan TG, Cryan JF, Cryan JF: **Anxiety, Depression, and the Microbiome: A Role for Gut Peptides**. *NEUROTHERAPEUTICS* 2018, **15**(1):36–59.
3. Sampson TR, Debelius JW, Thron T, Janssen S, Shastri GG, Ilhan ZE, Challis C, Schretter CE, Rocha S, Gradinaru V, et al. Gut Microbiota Regulate Motor Deficits and Neuroinflammation in a Model of Parkinson's Disease. CELL. 2016;167(6):1469–80.

4. Liu P, Wu L, Peng G, Han Y, Tang R, Ge J, Zhang L, Jia L, Yue S, Zhou K, et al. Altered microbiomes distinguish Alzheimer's disease from amnestic mild cognitive impairment and health in a Chinese cohort. BRAIN BEHAV IMMUN. 2019;80:633–43.
5. Heiss CN, Olofsson LE. The role of the gut microbiota in development, function and disorders of the central nervous system and the enteric nervous system. J NEUROENDOCRINOL. 2019;31(5):e12684.
6. Honda K, Littman DR. The microbiota in adaptive immune homeostasis and disease. NATURE. 2016;535(7610):75–84.
7. Bäumler AJ, Sperandio V. Interactions between the microbiota and pathogenic bacteria in the gut. NATURE. 2016;535(7610):85–93.
8. Kim S, Kwon S, Kam T, Panicker N, Karuppagounder SS, Lee S, Lee JH, Kim WR, Kook M, Foss CA, et al: **Transneuronal Propagation of Pathologic α-Synuclein from the Gut to the Brain Models Parkinson's Disease**. *NEURON* 2019, **103**(4):627–641.
9. Matheoud D, Cannon T, Voisin A, Penttinen A, Ramet L, Fahmy AM, Ducrot C, Laplante A, Bourque M, Zhu L, et al. Intestinal infection triggers Parkinson's disease-like symptoms in Pink1−/− mice. NATURE. 2019;571(7766):565–9.
10. Angelucci F, Cechova K, Amlerova J, Hort J. **Antibiotics, gut microbiota, and Alzheimer's disease**. *J NEUROINFLAMM* 2019, 16(1).
11. Rizzo R, Bortolotti D, Gentili V, Rotola A, Bolzani S, Caselli E, Tola MR, Di Luca D. KIR2DS2/KIR2DL2/HLA-C1 Haplotype Is Associated with Alzheimer's Disease: Implication for the Role of Herpesvirus Infections. J Alzheimers Dis. 2019;67(4):1379–89.
12. Garcez ML, Jacobs KR, Guillemin GJ. Microbiota Alterations in Alzheimer's Disease: Involvement of the Kynurenine Pathway and Inflammation. NEUROTOX RES. 2019;36(2):424–36.
13. Diling C, Tianqiao Y, Jian Y, Chaoqun Z, Ou S, Yizhen X. **Docking Studies and Biological Evaluation of a Potential β-Secretase Inhibitor of 3-Hydroxyhericenone F from Hericium erinaceus**. *FRONT PHARMACOL* 2017, 8.
14. Lai G, Guo Y, Chen D, Tang X, Shuai O, Yong T, Wang D, Xiao C, Zhou G, Xie Y, et al: **Alcohol Extracts From Ganoderma lucidum Delay the Progress of Alzheimer's Disease by Regulating DNA Methylation in Rodents**. *FRONT PHARMACOL* 2019, 10.
15. Chen DL, Zhang P, Lin L, Zhang HM, Deng SD, Wu ZQ, Ou S, Liu SH, Wang JY. Protective effects of bajijiasu in a rat model of Abeta(2)(5)(-)(3)(5)-induced neurotoxicity. J ETHNOPHARMACOL. 2014;154(1):206–17.
16. Chen D, Yang X, Yang J, Lai G, Yong T, Tang X, Shuai O, Zhou G, Xie Y, Wu Q. **Prebiotic Effect of Fructooligosaccharides from Morinda officinalis on Alzheimer's Disease in Rodent Models by Targeting the Microbiota-Gut-Brain Axis**. *FRONT AGING NEUROSCI* 2017, 9.
17. Dubois M, Lafaye De Micheaux P, Noël M, Valdois S. Preorthographical constraints on visual word recognition: Evidence from a case study of developmental surface dyslexia. COGN NEUROPSYCHOL. 2007;24(6):623–60.

18. Sun GZ, He YC, Ma XK, Li ST, Chen DJ, Gao M, Qiu SF, Yin JX, Shi J, Wu J. Hippocampal synaptic and neural network deficits in young mice carrying the human APOE4 gene. CNS NEUROSCI THER. 2017;23(9):748–58.
19. Tsilimigras MCB, Fodor AA. Compositional data analysis of the microbiome: fundamentals, tools, and challenges. ANN EPIDEMIOL. 2016;26(5):330–5.
20. Gao X, Williams SJ, Woodman OL, Marriott PJ. Comprehensive two-dimensional gas chromatography, retention indices and time-of-flight mass spectra of flavonoids and chalcones. J CHROMATOGR A. 2010;1217(52):8317–26.
21. Akiguchi I, Pallàs M, Budka H, Akiyama H, Ueno M, Han J, Yagi H, Nishikawa T, Chiba Y, Sugiyama H, et al. SAMP8 mice as a neuropathological model of accelerated brain aging and dementia: Toshio Takeda's legacy and future directions. NEUROPATHOLOGY. 2017;37(4):293–305.
22. Wang J, Xia Y, Grundke-Iqbal I, Iqbal K. Abnormal Hyperphosphorylation of Tau: Sites, Regulation, and Molecular Mechanism of Neurofibrillary Degeneration. J Alzheimers Dis. 2012;33(s1):123–39.
23. He X, Gong W, Zhang J, Nie J, Yao C, Guo F, Lin Y, Wu X, Li F, Li J, et al. Sensing and Transmitting Intracellular Amino Acid Signals through Reversible Lysine Aminoacylations. CELL METAB. 2018;27(1):151–66.
24. Walker JM, Dixit S, Saulsberry AC, May JM, Harrison FE. Reversal of high fat diet-induced obesity improves glucose tolerance, inflammatory response, β-amyloid accumulation and cognitive decline in the APP/PSEN1 mouse model of Alzheimer's disease. NEUROBIOL DIS. 2017;100:87–98.
25. Claesson MJ, Jeffery IB, Conde S, Power SE, O Connor EM, Cusack S, Harris HMB, Coakley M, Lakshminarayanan B, O Sullivan O, et al. Gut microbiota composition correlates with diet and health in the elderly. NATURE. 2012;488(7410):178–84.
26. Mazmanian SK, Liu CH, Tzianabos AO, Kasper DL: **An Immunomodulatory Molecule of Symbiotic Bacteria Directs Maturation of the Host Immune System**. *CELL* 2005, **122**(1):107–118.
27. Rincel M, Aubert P, Chevalier J, Grohard P, Basso L, Monchaux De Oliveira C, Helbling JC, Lévy É, Chevalier G, Leboyer M, et al. Multi-hit early life adversity affects gut microbiota, brain and behavior in a sex-dependent manner. Brain Behav Immun. 2019;80:179–92.
28. Li B, He Y, Ma J, Huang P, Du J, Cao L, Wang Y, Xiao Q, Tang H, Chen S. Mild cognitive impairment has similar alterations as Alzheimer's disease in gut microbiota. Alzheimer's Dement. 2019;15(10):1357–66.
29. Zhuang Z, Shen L, Li W, Fu X, Zeng F, Gui L, Lü Y, Cai M, Zhu C, Tan Y, et al. Gut Microbiota is Altered in Patients with Alzheimer's Disease. J Alzheimers Dis. 2018;63(4):1337–46.
30. Swanson KV, Deng M, Ting JP. The NLRP3 inflammasome: molecular activation and regulation to therapeutics. Nat Rev Immunol. 2019;19(8):477–89.
31. Gukovskaya AS, Gukovsky I, Algül H, Habtezion A. Autophagy, Inflammation, and Immune Dysfunction in the Pathogenesis of Pancreatitis. GASTROENTEROLOGY. 2017;153(5):1212–26.
32. Heckmann BL, Teubner BJW, Tummers B, Boada-Romero E, Harris L, Yang M, Guy CS, Zakharenko SS, Green DR. LC3-Associated Endocytosis Facilitates β-Amyloid Clearance and Mitigates

Neurodegeneration in Murine Alzheimer’s Disease. CELL. 2019;178(3):536–51.

33. Saxton RA, Sabatini DM: **mTOR Signaling in Growth, Metabolism, and Disease**. *CELL* 2017, **168**(6):960–976.
34. Toledo JB, Arnold M, Kastenmüller G, Chang R, Baillie RA, Han X, Thambisetty M, Tenenbaum JD, Suhre K, Thompson JW, et al. Metabolic network failures in Alzheimer's disease: A biochemical road map. Alzheimer's Dement. 2017;13(9):965–84.
35. Bellono NW, Bayrer JR, Leitch DB, Castro J, Zhang C, O Donnell TA, Brierley SM, Ingraham HA, Julius D: **Enterochromaffin Cells Are Gut Chemosensors that Couple to Sensory Neural Pathways**. *CELL* 2017, **170**(1):185–198.
36. Rothhammer V, Borucki DM, Tjon EC, Takenaka MC, Chao CC, Ardura-Fabregat A, de Lima KA, Gutierrez-Vazquez C, Hewson P, Staszewski O, et al. Microglial control of astrocytes in response to microbial metabolites. NATURE. 2018;557(7707):724–8.
37. Pistollato F, Sumalla Cano S, Elio I, Masias Vergara M, Giampieri F, Battino M. Role of gut microbiota and nutrients in amyloid formation and pathogenesis of Alzheimer disease. NUTR REV. 2016;74(10):624–34.

Figures

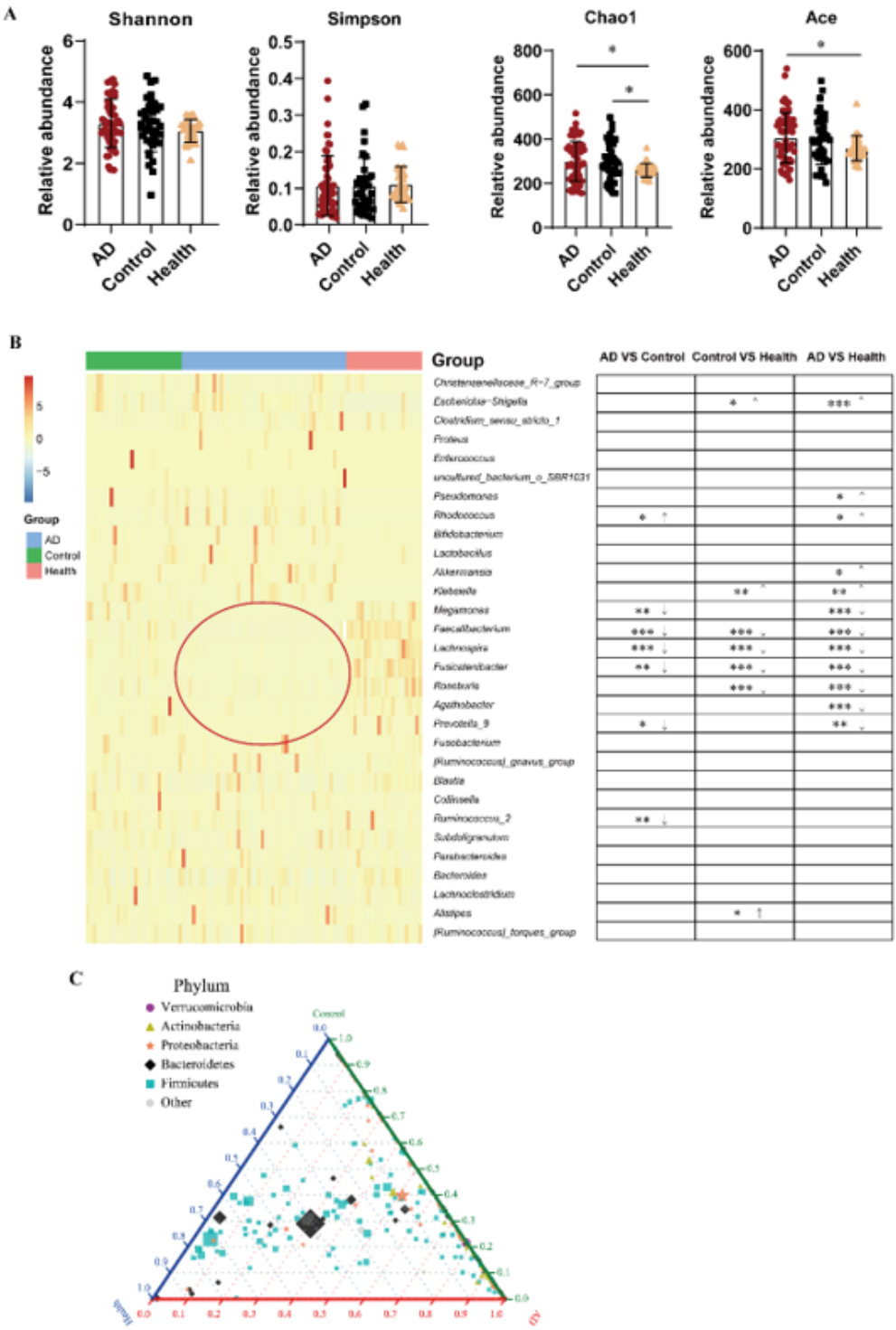

Figure 1

Variation characteristics of gut microbiota in AD patients. (A) Alpha diversity analysis results; (B) Changes in the gut microbiota at the genus level and Statistical chart of some bacterial of genus level; (C) Three-phase diagram of gut microbiota structure (at phylum level) in AD patients. Feces was collected from 48 AD patients, 28 disease controls, and 26 healthy controls. The 16S rRNA analysis showed

significant differences for the abundance-based covered estimator (ACE) and Chao 1 indexes from the healthy groups ($p < 0.05$). (* denote $p < 0.05$, ** denote $p < 0.01$, *** denote $p < 0.001$)

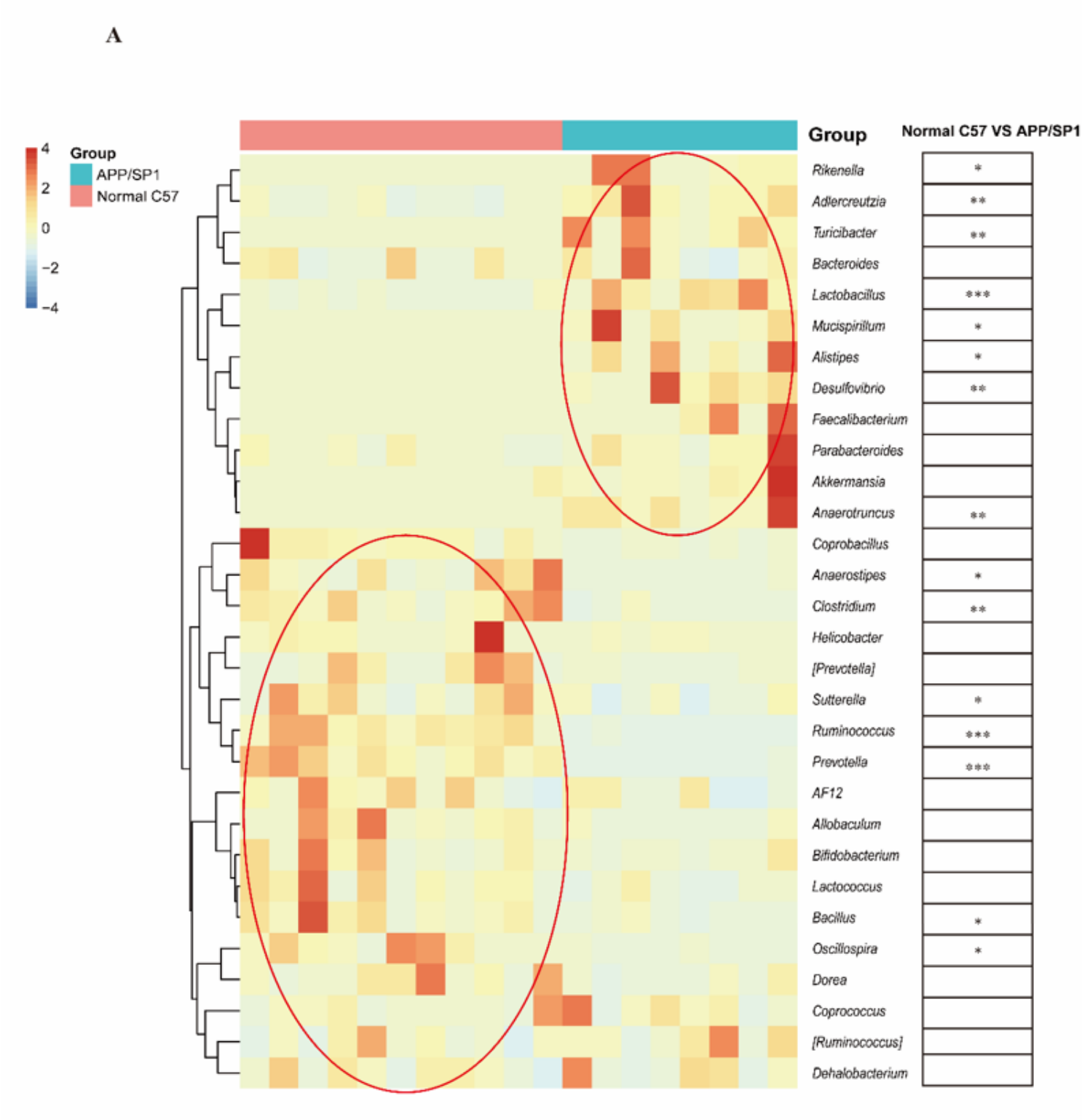

Figure 2

The gut microbiota composition of APP/SP1 mice. (A) The heatmap of gut microbiota at the genus level and Statistical chart of some bacterial of genus level. The gut microbiota composition of APP/PS1 mice using 16S rRNA sequencing, and the results revealed that the gut microbiota composition of APP/PS1

mice (n = 8) were very different from the normal C57 mice (n = 11). (* denote p < 0.05 , ** denote p < 0.01, *** denote p < 0.001)

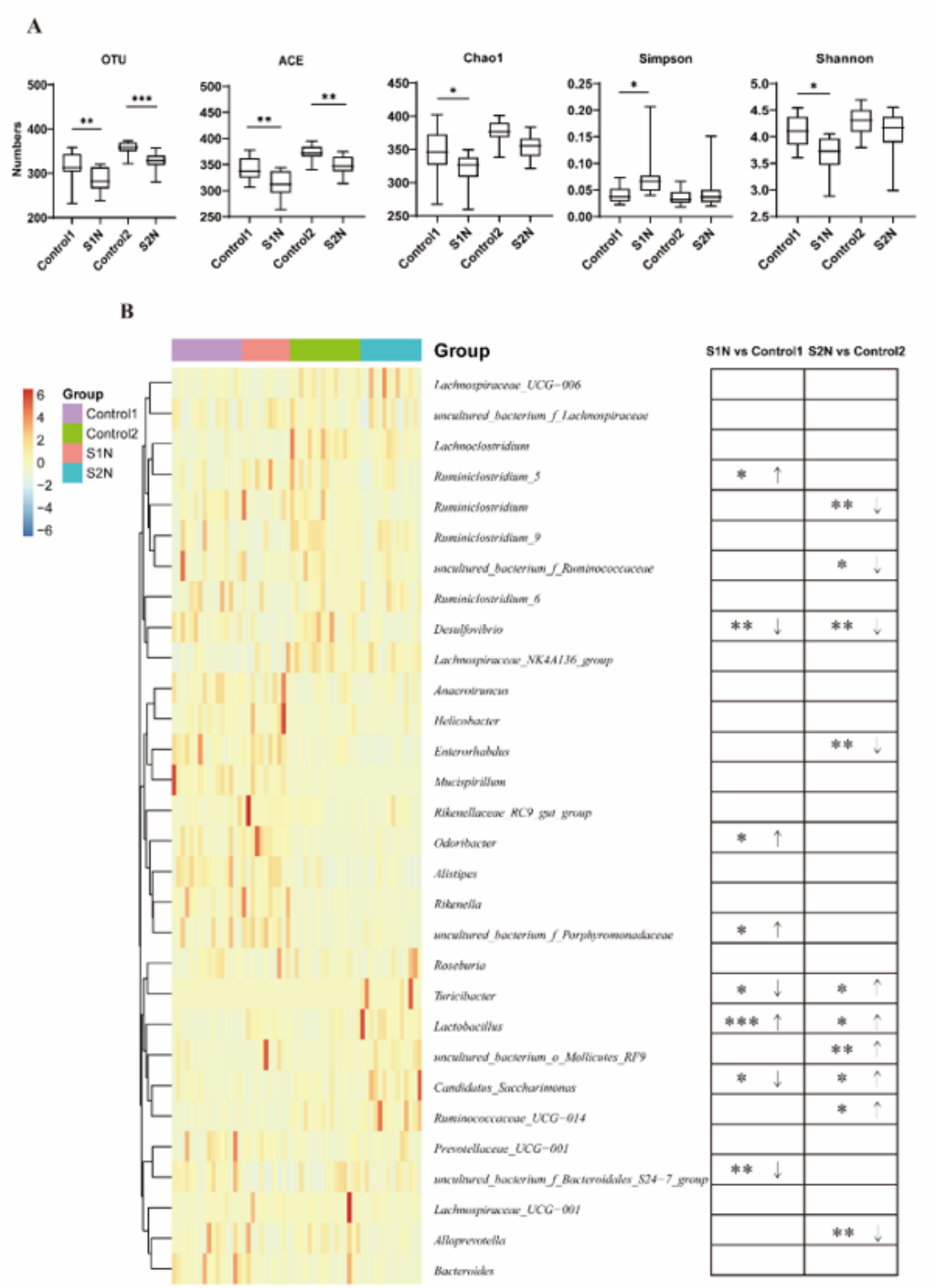

Figure 3

Colonization of gut microbiota analysis after AD-cohousing. (A) Alpha diversity analysis results; (B) Changes in the gut microbiota at the genus level and Statistical chart of some bacterial of genus level. After 2 weeks of pregnancy, the dams were placed with two 8-month-old APP/PS1. The mice were

cohoused until 14 days after birth, and at first and second month time points, the gut microbiota composition of intestinal contents were analyzed using 16S rRNA sequencing. S1N denote cohousing mice at first month time point. S2N denote cohousing mice at second month time point. AD-cohousing denote cohousing mice at tenth month time point.

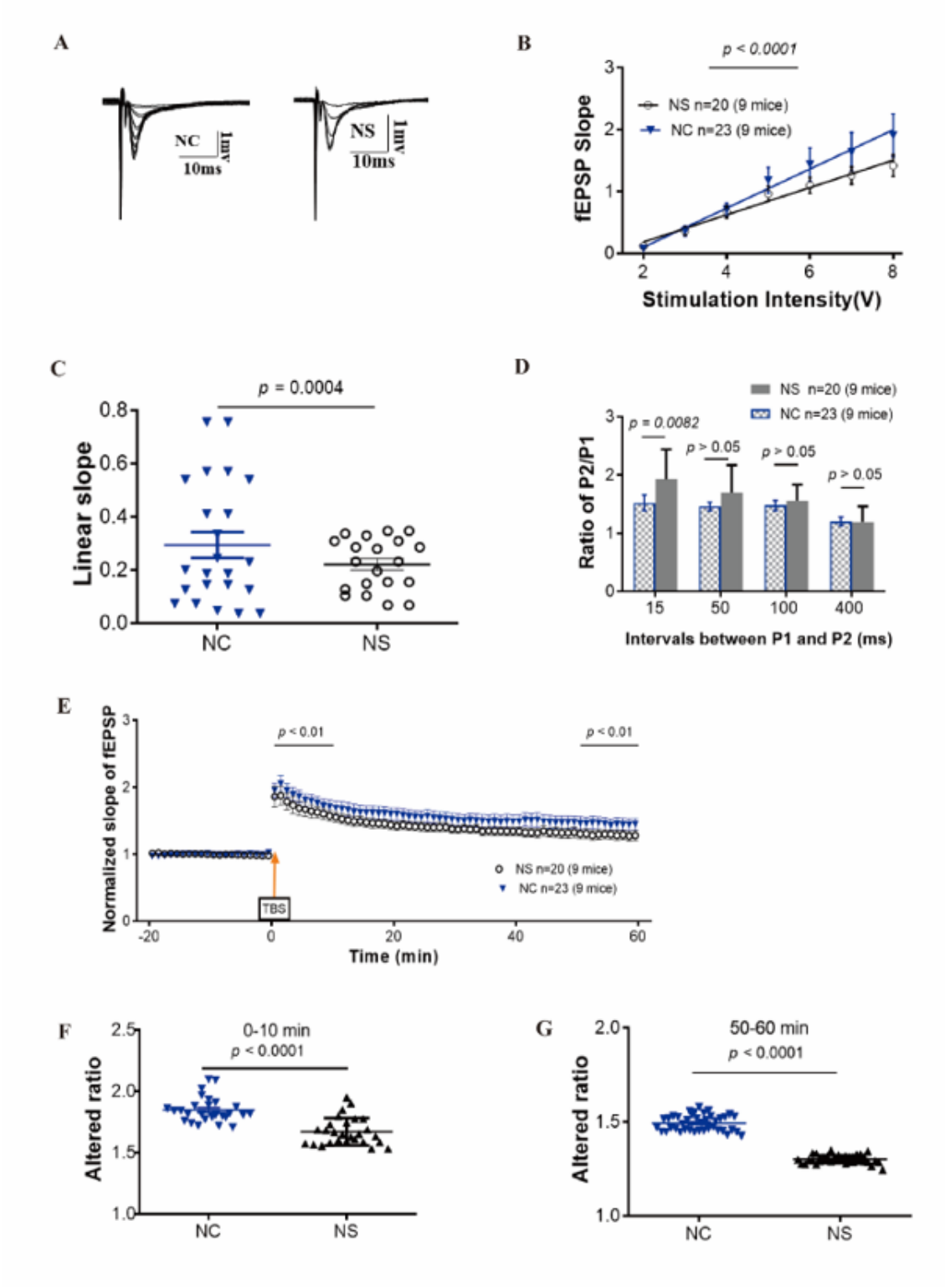

Figure 4

LTP in hippocampal slices after cohousing. Ten months later, subsets of mice were randomly selected to perform standard field potential recordings. (A)Repetitive stimulation (0.33 Hz) of Schaffer collaterals evoked fEPSPs in the hippocampal CA1 region. (B)The input-output relationship curves (C) Linear slopes revealed that compared to control mice (NC), the hippocampal CA1 neurons of AD-cohousing mice showed decreased excitability ($p < 0.05$, unpaired t test). (D) Synaptic short-term plasticity was measured using a PPF protocol in hippocampal slices. Statistical analyses from all slices demonstrated a significant inhibition of the ratio of P2/P1 at all tested P1 and P2 intervals in AD-cohousing mice compared to control mice of NC. (E)The plot recording time to normalized fEPSP slopes (baseline as 1) from pooled data showed impaired LTP induction (after theta-burst stimulation 0-10 min) and maintenance (after theta-burst stimulation 50-60 min) in all treated groups. ($p < 0.05$, unpaired t test) (G) The mean LTP induction results after theta-burst stimulation 0-10 min. ($p < 0.05$, unpaired t test). (F) The mean LTP induction results after theta-burst stimulation 50-60 min. ($p < 0.05$, unpaired t test). Data are presented as the means ± SD of more than 6 independent experiments. *$p < 0.05$ and **$p < 0.01$ vs. the model group by one-way ANOVA, followed by the Holm-Sidak test. (NC denote the control group, NS denote the AD-cohousing group)

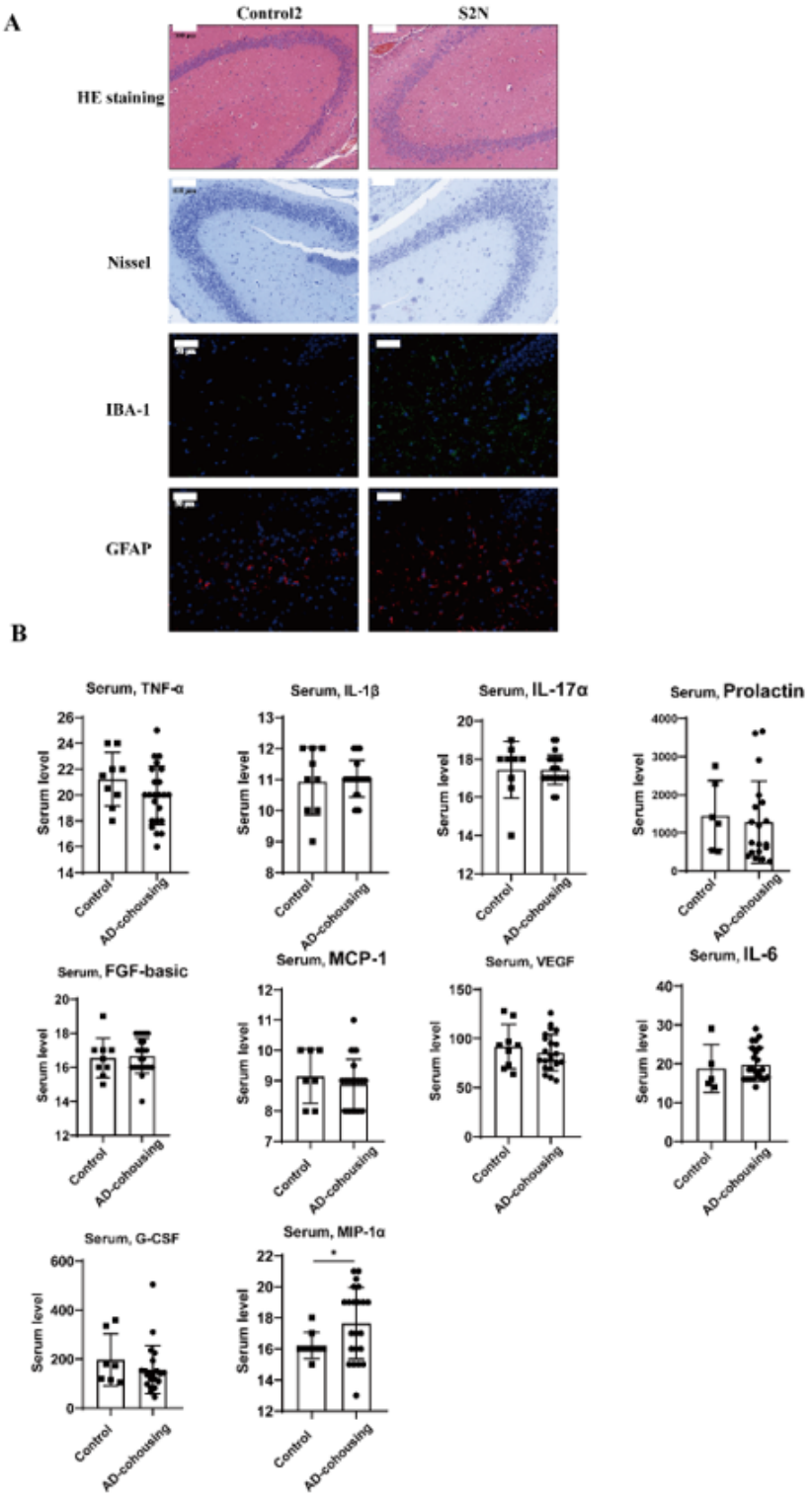

Figure 5

AD-cohousing enhances inflammation in brain and serum. (A) Brain sections were processed for H&E, Nissl staining, Immunofluorescent labeling of microglial IBA-1, and GFAP in the CA1 area. (B) The serum levels of MIP-1α were changed after AD-cohousing ($p<0.05$, $n>6$). Data are presented as the means ± SD of more than 8 independent experiments. (*$p < 0.05$, unpaired t test)

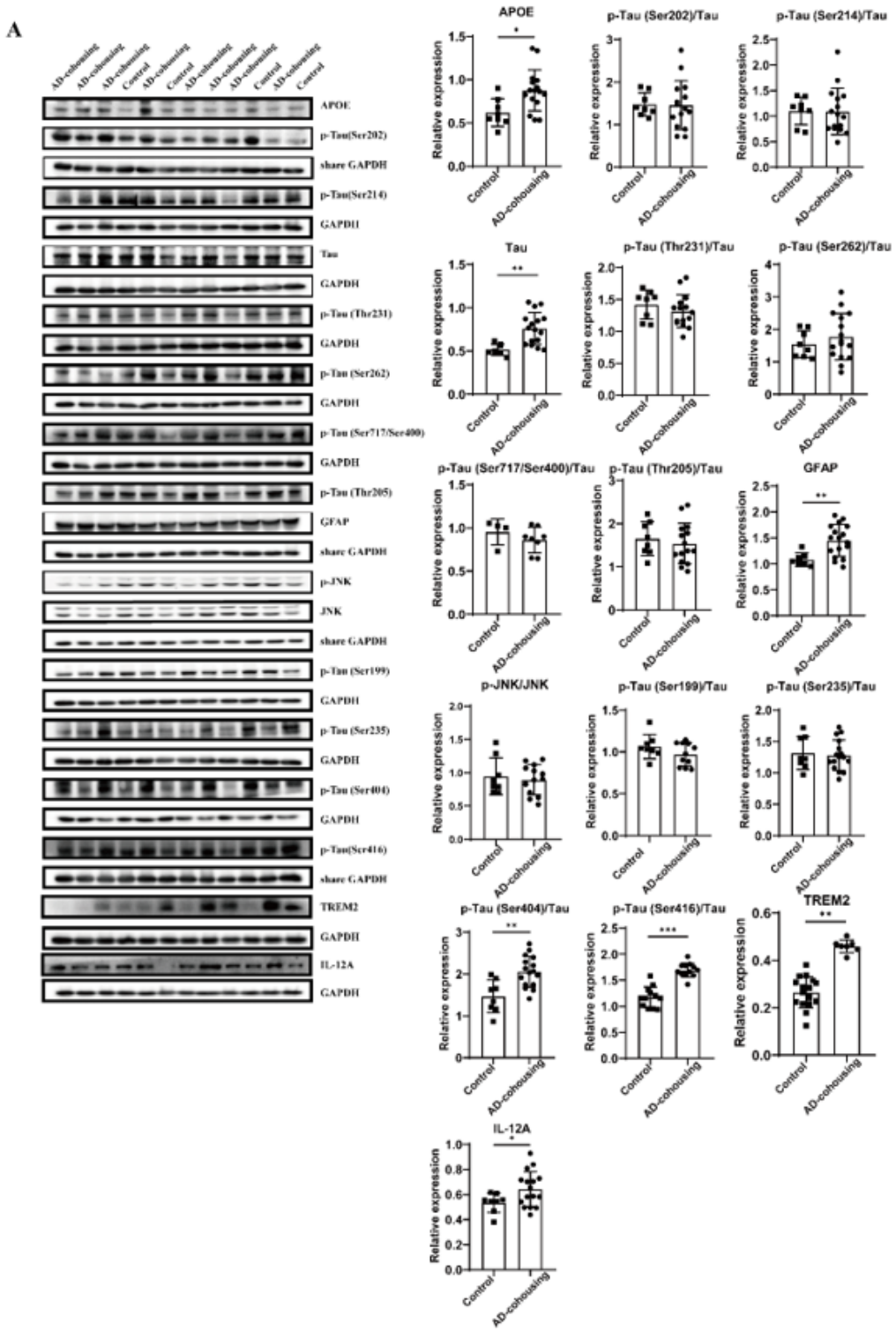

Figure 6

AD-cohousing accelerates Tau protein hyperphosphorylation, increase inflammation, induce autophagy and increase inflammation in brain tissue AD biomarkers of Tau, Aβ4, p-Tau, BACE, and APOE; and different phosphorylation sites of Tau protein at -Ser404 and -Ser416 were upregulated after cohousing. The autophagy biomarkers of LC3A/B, Atg14, AKT, ATG14,ATG12, mTOR ,CRTC1, CRTC2 and PI3K p85 in AD-cohousing mice brain tissue. TLR4, TREM2, IL-12α, IL-23, NLRP3 were upregulated after cohousing

Data are presented as the means ± SD of more than 8 independent experiments. (*p < 0.05 and **p < 0.01, unpaired t test)

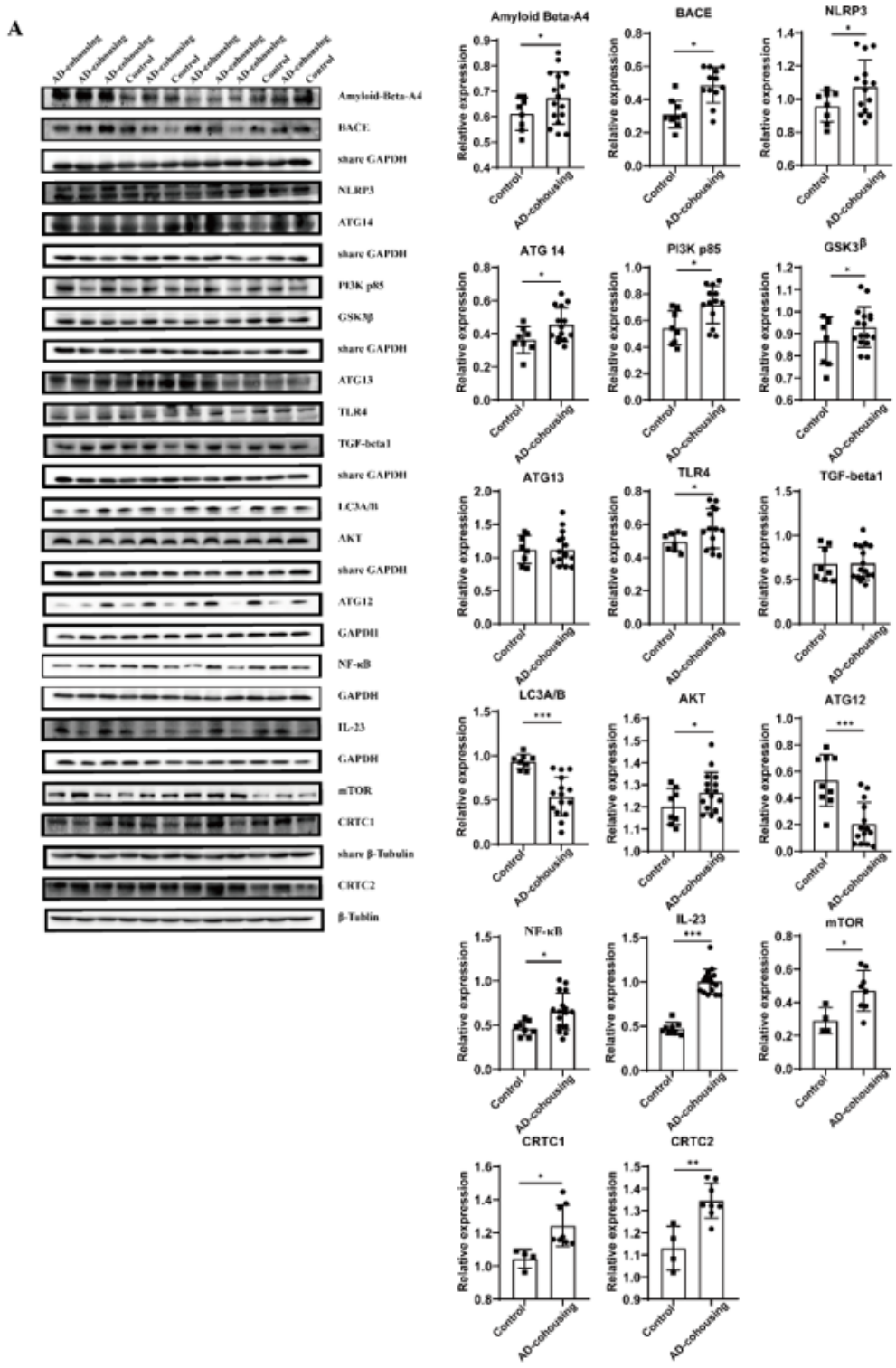

Figure 7

AD-cohousing accelerates Tau protein hyperphosphorylation, increase inflammation, induce autophagy and increase inflammation in brain tissue AD biomarkers of Tau, Aβ4, p-Tau, BACE, and APOE; and different phosphorylation sites of Tau protein at -Ser404 and -Ser416 were upregulated after cohousing.

The autophagy biomarkers of LC3A/B, Atg14, AKT, ATG14,ATG12, mTOR ,CRTC1, CRTC2 and PI3K p85 in AD-cohousing mice brain tissue. TLR4, TREM2, IL-12α, IL-23, NLRP3 were upregulated after cohousing Data are presented as the means ± SD of more than 8 independent experiments. (*p < 0.05 and **p < 0.01, unpaired t test)

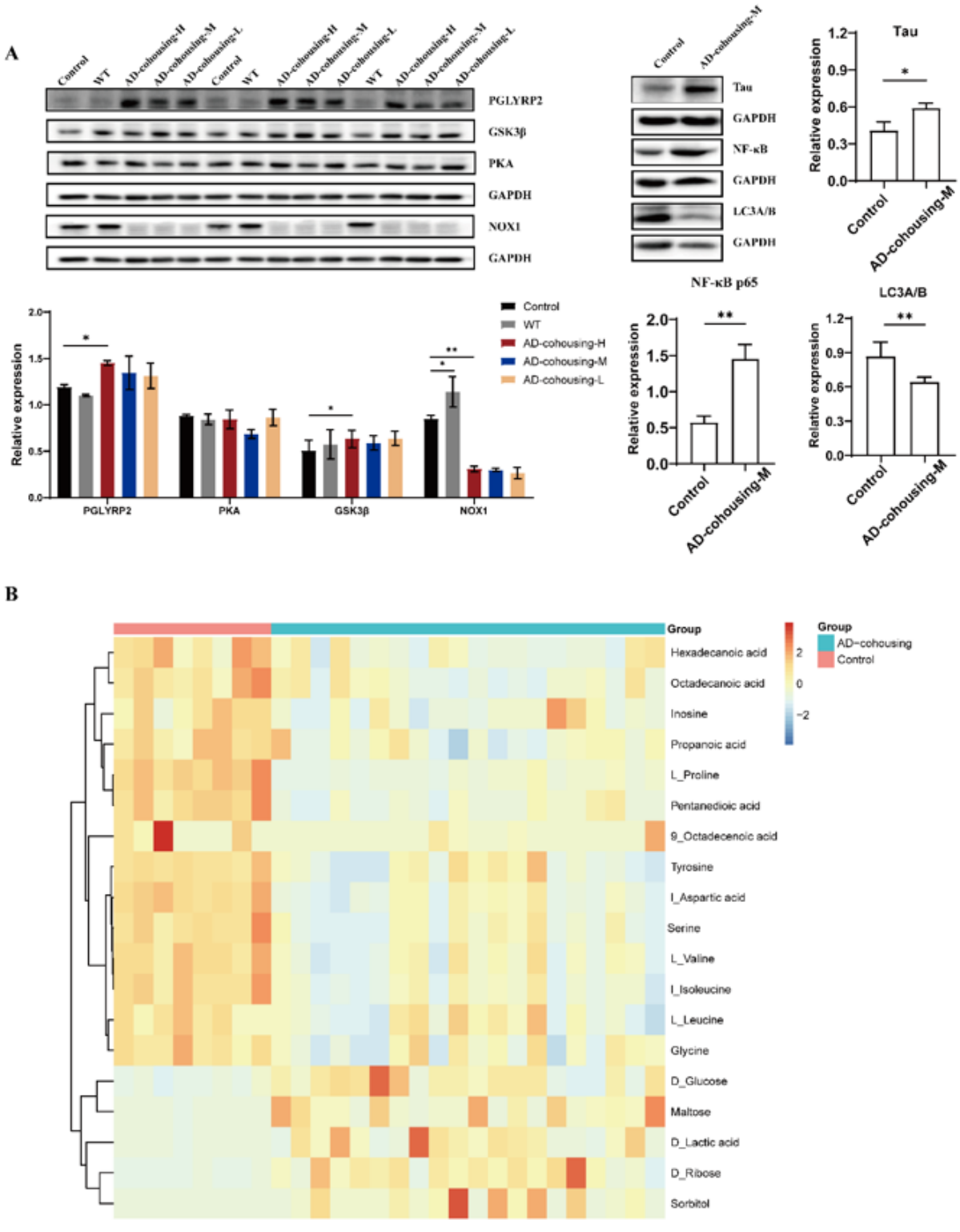

Figure 8

Fecal metabolites induce inflammation and autophagy in BV2 cells and Heatmap of different metabolites of intestinal contents in AD-cohousing mice (A)Factors of fermentation products of some pathogenic and conditioned pathogens, or fermentation products of some diet compounds with AD gut microbiota, on the expressions the proteins of Tau, GSK3β, NF-κB p65, LC3A/B; PGLYRP2 and NOX1 levels were altered by extracts of AD-cohousing mice feces (17.25 mg/ml high dose, AD-cohousing-H; 13.5 mg/ml of middle dose, AD-cohousing-M; and 7.7mg/ml low dose, AD-cohousing-L;13.5 mg/ml of middle dose, Control). The culture conditions of the WT group were the same as those of the other groups, but without any treatment. Data are presented as the means ± SD of more than 3 independent experiments. (*$p < 0.05$ and **$p < 0.01$) (B) Heatmap of different metabolites of intestinal contents in AD-cohousing mice.(control group, n=8; cohousing group, n=20)

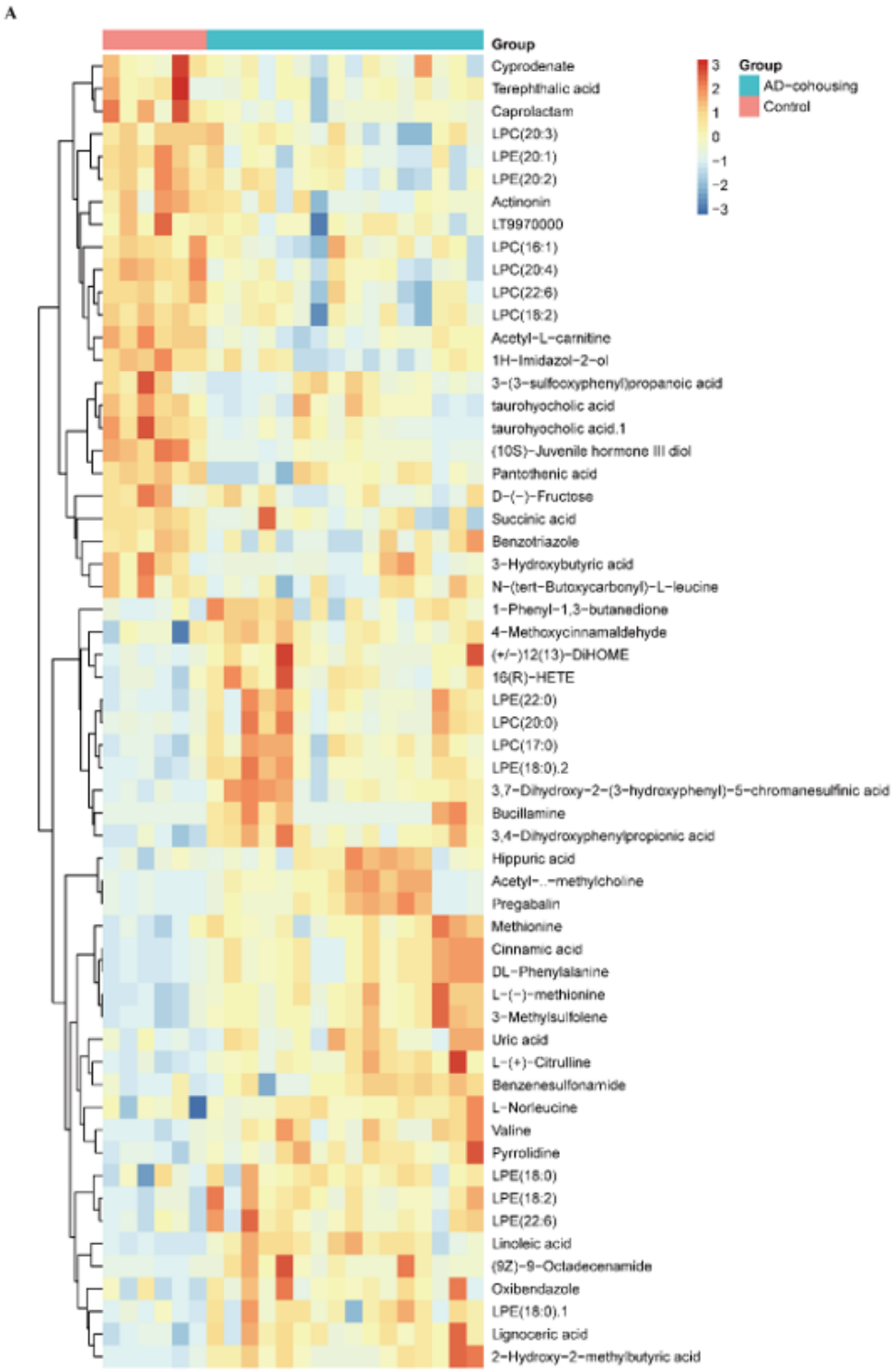

Figure 9

Metabolomics analysis of serum in AD-cohousing mice. (A) Heatmap of metabolomics analysis of serum in AD-cohousing mice.(control group, n=6; cohousing group, n=16)

Supplementary Files

This is a list of supplementary files associated with this preprint. Click to download.

- SupplementalInformation.docx